ACS APPLIED MATERIALS & INTERFACES

Research Article

www.acsami.org

Protein-Decorated Reduced Oxide Graphene Composite and its Application to SERS

Fei Lu, Shaohua Zhang, Hejun Gao, Han Jia, and Liqiang Zheng*

Key Laboratory of Colloid and Interface Chemistry, Shandong University, Ministry of Education, Jinan, 250100, P. R. China

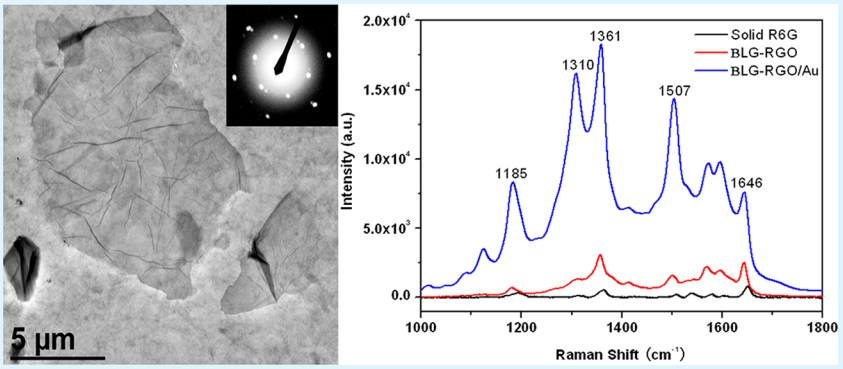

ABSTRACT: A globular protein, β-lactoglobulin (BLG), was used to decorate reduced graphene oxide sheets (RGO) and the obtained BLG-RGO composite can be dispersed in aqueous solution with pH-sensitive solubility. The morphology of the BLG-RGO composite was studied by transmission electron microscopy (TEM) and atomic force microscopy (AFM). The results indicate that BLG-RGO is effectively exfoliated with an average thickness of 2.5 nm. UV−vis spectra were performed to examine the reduction degree and determine the optimum concentration of β-lactoglobulin and appropriate pH value. Furthermore, Raman spectra demonstrate that β-Lactoglobulin promotes the chemical reduction process of graphene oxide and benefits to repair the crystal defects. Due to the adsorption of β-Lactoglobulin on the surface of graphene sheets, the BLG-RGO composite was further used as template for Au nanoparticles assembly. These Au nanoparticles assembled on the BLG-RGO composite were shown to yield a large SERS enhancement for Rhodamine 6G.

KEYWORDS: *reduced graphene oxide, β-lactoglobulin, composite, pH-sensitive solubility, Au nanoparticles, SERS*

INTRODUCTION

Graphene, a single-atom-thick sheet of graphite, has attracted an increasing attention in recent years since its discovery in 2004 by Geim and co-workers.[1] This is mainly due to the atomic two-dimensional structure of graphene and its excellent mechanical, thermal, and electrical properties.[2−4] The unique properties of graphene sheets provide potential application in various fields including dye-sensitized solar cells,[5] field effect transistors,[6] lithium ion batteries[7] and biosensors.[8,9] Up-to-date, various effective techniques have been developed for producing graphene, such as mechanical cleavage of graphite,[1] epitaxial growth,[10,11] chemical vapor deposition,[12,13] and reduction of graphite oxide.[14] However, the high specific surface area of graphene sheets makes them tend to form irreversible aggregation by van der Waals interaction, which restricts the large scale application of graphene sheets.[15] Thus, the functionalization and modification of graphene to improve the dispersity and solubility will be significantly critical.

Considerable efforts have been devoted to modify the graphene through covalent and noncovalent methods.[16−20] Unfortunately, covalent method may leave some sp^3 carbons in graphene structure due to the covalent linkage, resulting in the decrease of the electrical properties of graphene. Thus noncovalent interaction is playing an increasingly important role in the decoration of graphene. Like the dispersion of carbon nanotubes, traditional surfactants such as sodium sulfate (SDS) and sodium dodecylbenzene sulfonate (SDBS) can be used to disperse graphene sheets in aqueous solutions.[21] Didodecylmethylammonium bromide (DDAB) can also be exploited to disperse graphene sheets in aqueous solution and then transfer them into the organic phase.[22] The graphene sheets decorated by some aromatic electroactive dyes such as Congo red and Brilliant blue were found to perform wide solubility in water, dimethysulfoxide (DMSO), *N,N* -dimethyl-formamide (DMF), methanol, ethanol, and other organic solvents.[23,24] Moreover, polymer-coated graphene sheets by poly (1-vinyl-3-ethylimidazolium) salts and poly (1-vinyl-3-butylimidazolium) salts can also be well dispersed in water, organic solvents and even ionic liquids.[25,26] Although stable graphene dispersions can be obtained through these approaches, the harsh chemical treatment reduces the possibility for the application of graphene sheets in the living

Received: April 11, 2012
Accepted: June 12, 2012
Published: June 12, 2012

system.[27] Consequently, DNA and proteins, as atoxic and biocompatible molecules, attract increasing attention to decorate graphene sheets for the potential biological applications.[28,29]

β-Lactoglobulin, from milk of several mammals, is a globular protein with 162 amino acid residues with different hydrophilicity and both α-helices and β-sheets in its secondary structure.[30] This complex amphiphilic biopolymer has been widely studied on its adsorption onto solid surface by experimental works and molecular simulations.[31,32] In this work, we used β-lactoglobulin as a stabilizer to prepare reduced graphene oxide (RGO) dispersion from graphene oxide (GO) solution. Our strategy is to obtain BLG-RGO composite with β-Lactoglobulin at an optimum concentration and a suitable pH value. Then the obtained BLG-RGO conjugate was further used as a general template for the efficient assembly of Au nanoparticles.

EXPERIMENTAL SECTION

Preparation of Graphene Oxide. Graphene oxide (GO) was synthesized from graphite powders (Aladdin) via the well-known Hummers method.[33] Five grams of graphite powders, 3.75 g of sodium nitrate, and 170 mL of sulfuric acid (98%) were mixed together and stirred strongly at 0 °C for 15 min in a 1000 mL reaction beaker immersed in an ice bath. Then 25 g of potassium permanganate was added gradually to the above mixture with incessant stirring to keep the temperature of the suspension from exceeding 20 °C. After the mixture was stirred continuously for 2 h, the ice bath was removed to allow the temperature of this suspension to rise to 35 °C. At the end of another 50 min stirring, 250 mL of distilled water was added slowly. Then the temperature increased to 98 °C and the mixture was maintained at this temperature for 15 min. Then the suspension was treated with 170 mL of 30% H_2O_2 to reduce residual permanganate ions to manganese ions until the gas evolution ceased. After that, 750 mL of distilled water was added. The products were filtered, washed with distilled water and dried at 100 °C in vacuum for 24 h to obtain the dark brown GO plates.

Preparation of β-Lactoglobulin Stabilized Reduced Graphene Oxide Solution. The GO suspension of 1 mg/mL was prepared by the above GO plates under bath ultrasonication for 30 min. Then the suspension was centrifugated at 4000 rpm for 10 min to remove the unoxidized thick graphite flakes. A specific amount of β-Lactoglobulin and 0.2 mL of hydrazine hydrate were added to 5 mL of the above GO solution, and the pH value of the solution was adjusted to 12 by 1 M NaOH solution. The concentration of β-Lactoglobulin in the final solution varied from 0.25 mg/mL, 0.5 mg/mL, 1.0 mg/mL to 2.0 mg/mL. Then the solution was heated at 80 °C for 24 h following the centrifugation at 4000 rpm for 10 min to obtain the BLG-RGO solution.

Preparation of BLG-RGO/Au Nanoparticle Hybrid. Four milliliters of BLG-RGO aqueous solution and 1.0 mL of $HAuCl_4$ (0.1 M) solution were mixed together at room temperature. Then, 1.0 mL of $NaBH_4$ solution (0.1 M) was added and the mixture was stirred for 5 min. The obtained BLG-RGO/Au nanoparticle composite was purified by centrifugation, washed thoroughly with distilled water.

Characterization. The BLG-RGO solution was evaluated by UV–vis spectrophotometer (U-4100, Hitachi, Japan), with a wavelength range from 200 to 600 nm. Before measurements, each sample was diluted by distilled water to the concentration of one-fiftieth of its initial concentration. The corresponding β-Lactoglobulin solution with the same concentration and pH value was settled as blank. FT-IR spectroscopy was carried out on a PerkinElmer LS-55 spectrophotometer (PE Co., UK). Transmission electron microscopy (TEM) observations and selected area electron diffraction (SAED) patterns were achieved on a JEOL JEM-100 CXII (Japan) transmission electron microscope with an accelerating voltage of 80 kV. Atomic force microscopy (AFM) observations were conducted on a Nanoscope III A (U.S.A.) atomic force microscope by the tapping mode with very dilute BLG-RGO solution dropped on a silicon plate. Raman spectra were recorded from 500 cm^{-1} to 2000 cm^{-1} on a confocal microprobe Raman spectrometer (Jobin-Yvon HR800) using a 633 nm helium–neon laser.

SERS Measurements. SERS measurements were carried out on a confocal microprobe Raman spectrometer (Jobin-Yvon HR800). The reference sample was prepared by drop-casting 100 μL of 1.0×10^{-4} M R6G aqueous solution onto a quartz substrate and dried in atmosphere. Samples for SERS were prepared by drop-casting 100 μL of 1.0×10^{-4} M R6G aqueous solution and 100 μL BLG-RGO composite solution or 100 μL BLG-RGO/Au hybrid solution onto a quartz substrate. The SERS measurements were conducted with an excitation wavelength of 633 nm and power of 20 mW. Spectra were collected by focusing the laser line onto the sample using a 50× objective, providing a spatial resolution of about 1 μm. The data acquisition time was 10 s for one accumulation. Measurements at different positions were carried out for each sample to test the reproducibility.

RESULTS AND DISCUSSION

Dispersive Properties of BLG-RGO Composite. Figure 1 shows the photographs of GO, RGO and BLG-RGO solutions.

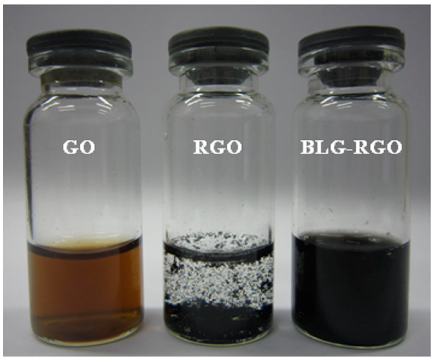

Figure 1. Photographs of the GO, RGO, and BLG-RGO aqueous solutions.

All of the solutions were placed for one week before taking the photograph. It is obvious that GO can be well dispersed in water without any dispersants. This phenomenon should be attributed to the electrostatic repulsion of GO sheets, as a result of ionization of the carboxylic acid and phenolic hydroxyl group existing on the GO sheets.[34,35] However, most oxygen-containing groups of GO are removed and the π-electron conjugation within the aromatic system is partially restored after the reduction. So RGO aggregates into irregular particles due to the high hydrophobic interaction and π–π stacking, which severely restricts its further application.[36,37] Amazingly, no aggregation was found in the solution of RGO obtained in the presence of β-lactoglobulin and this BLG-RGO dispersion was stable and homogeneous for more than two months.

To better represent the individual state of graphene sheets, TEM and AFM investigations were conducted. Figure 2a shows the TEM image of BLG-RGO composite with the inset showing the SAED pattern. Apparently, the BLG-RGO sheets are thin and transparent with some pleats on the surface. The SAED pattern of BLG-RGO sheets shows strong diffraction spots with six-folded rotational symmetry which clearly indicate the graphic crystalline structure. The inner diffraction spots are corresponding to (100) planes and the outer diffraction spots are related to (110) planes.[29,38] Furthermore, the intensity of the inner and outer diffraction spots is nearly the same, as a feature of single- or few-layer-stacking graphene sheets. AFM

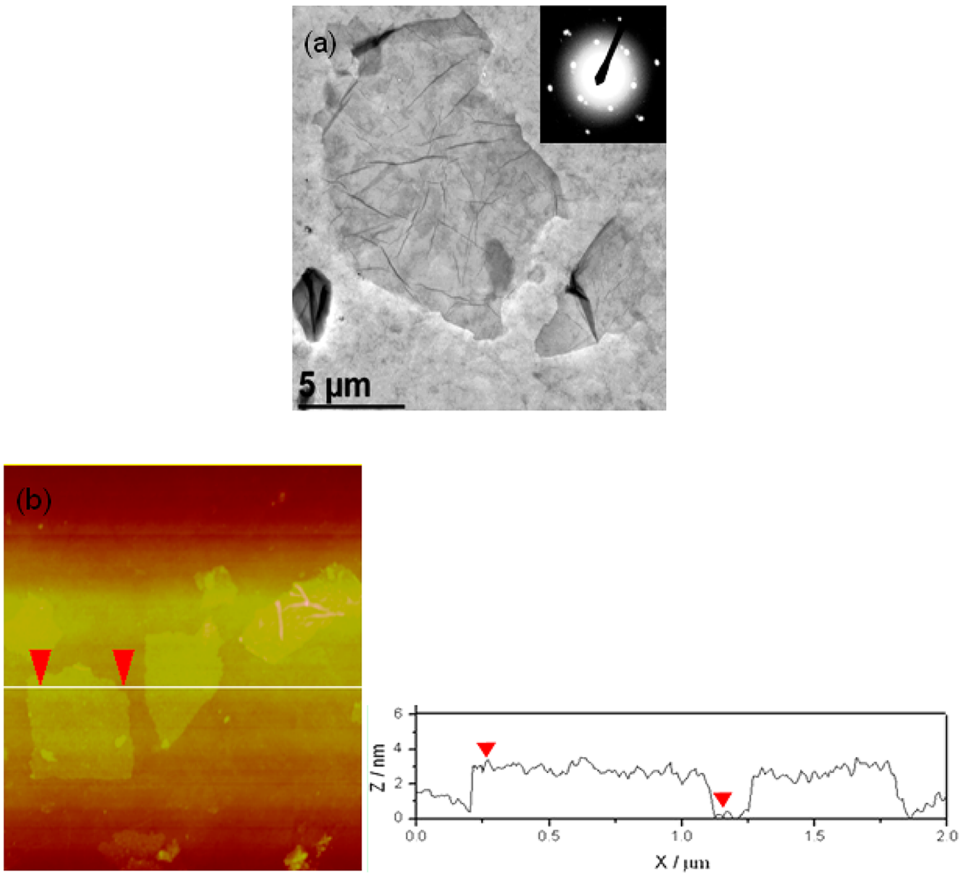

Figure 2. (a) TEM image of BLG-RGO composite and the inset picture showing the SAED pattern of BLG-RGO sheets. (b) Topography and height profile AFM images of BLG-RGO sheets. All samples were fabricated from the same BLG-RGO solution with 0.5 mg/mL β-lactoglobulin.

observation can further demonstrate the results. As shown in Figure 2b, the thickness of BLG-RGO sheets ranges from 2.5 to 3.0 nm, slightly higher than the common monolayer graphene sheets obtained from aqueous solution (1.2 nm).[18] Considering the adsorbed β-lactoglobulin molecules on one side of the graphene sheets to contribute about 2 nm,[39−41] it is reasonable to assume that the obtained RGO sheets are almost monolayered. Both visual observations of TEM and AFM indicate that RGO sheets can be dispersed by β-lactoglobulin with a stable one-layered state in aqueous solution.

Spectral Characterization of BLG-RGO Composite. The β-lactoglobulin functionalized RGO sheets were investigated by FT-IR spectroscopy to determine the formation of BLG-RGO composite. Figure 3 shows the FT-IR spectra of GO, RGO, β-lactoglobulin, and BLG-RGO composite. The C═O of carboxylic acid at 1728 cm^{-1} and C−O of epoxide at 1051 cm^{-1} are present in the spectrum of GO. The peak at 1626 cm^{-1} can be assigned to the skeletal vibrations of unoxidized graphitic domains or stretching deformation vibration of intercalated water.[42] For the RGO sample, the peaks of oxygen-containing groups gradually decrease after reduction and the new peak at 1572 cm^{-1} can be ascribed to the C═C stretching vibration of RGO restored conjugate structure.[43] The spectrum for β-Lactoglobulin contains two typical peaks: amide I band at 1658 cm^{-1} (mainly C═O stretching) and amide II band at 1548 cm^{-1} (C−N stretching).[44,45] These two bands can still be observed in the spectrum of BLG-RGO, indicating that RGO is successfully decorated by β-lactoglobulin.

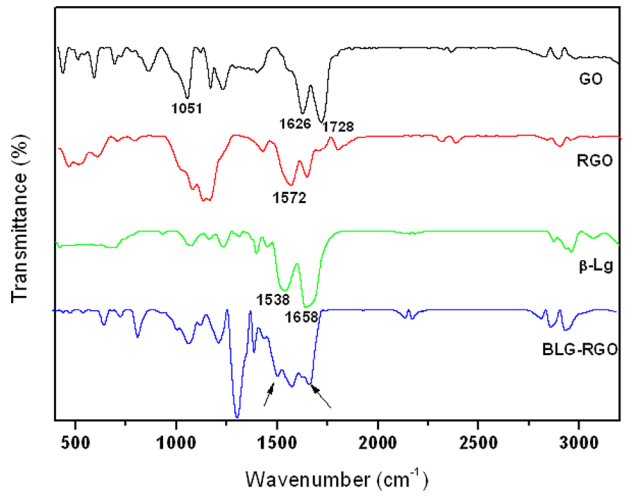

Figure 3. FT-IR spectra of GO (black curve), RGO (red curve), β-lactoglobulin (green curve), and BLG-RGO (blue curve).

UV−vis spectroscopy is a common method to monitor the degree of reduction and the concentration of RGO in the solution. As shown in Figure 4, the GO solution exhibits an UV−vis absorption peak at 229 nm (assigned to the $\pi-\pi^*$ transitions of aromatic C−C bonds) and a shoulder at 304 nm (assigned to the n-π^* transitions of C═O bonds).[46] After the reduction process, the π-conjugated network of graphene has been partial restored. So the absorption peak for the RGO sample shows a red shift to 261 nm.[47] Furthermore, it is

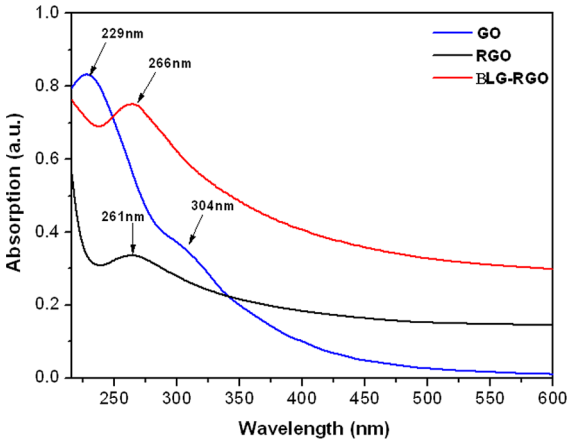

Figure 4. UV−vis spectra of the supernatant of GO (black curve), RGO (red curve), and BLG-RGO with 0.5 mg/mL β-lactoglobulin (blue curve).

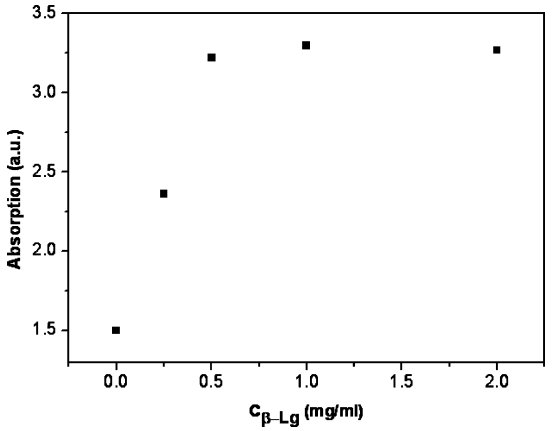

Figure 5. UV−vis absorption of BLG-RGO solutions at 266 nm with different concentrations of β-Lactoglobulin as 0, 0.25, 0.5, 1.0, and 2.0 mg/mL.

obvious that the absorption intensity of RGO is relatively low due to the small amount of remaining RGO sheets in the solution. However, much more red shift to 266 nm and stronger absorption intensity are observed for the BLG-RGO sample, as an evidence of higher reduction degree and larger graphene concentration with the aid of β-lactoglobulin in the solution.

β-Lactoglobulin is a protein containing 162 amino acid residues with different hydrophilicities.[30] Among these residues, hydrophobic groups and aromatic groups from tyrosine, tryptophan or other amino acid, are expected to interact with the RGO surface through hydrophobic interaction and $\pi-\pi$ stacking. Also, β-lactoglobulin has many charged residues with strong hydrophilicity to make it easily dissolved in water. Considering β-lactoglobulin has both hydrophobic and hydrophilic groups, β-Lactoglobulin molecules can be adsorbed on the surface of graphene sheets due to hydrophobic interaction and $\pi-\pi$ stacking while the hydrophilic groups are oriented toward the aqueous phase.[23,29] This interaction reduced the surface energy of the graphene sheets, and thus the obtained BLG-RGO composite can maintain isolated state stably in water.

The UV−vis absorbance of BLG-RGO solutions with increasing concentrations of β-Lactoglobulin from 0.25 mg/mL to 2.0 mg/mL was also obtained. The absorption peaks in the spectra present a little difference in wavelength but significant changes in intensity. According to the Lambert−Beer's law, the absorbance of graphene will be increased linearly with the increasing amount of graphene sheets in the solution. So the absorbance at 266 nm was recorded to compare the concentration of BLG-RGO in the solution. Figure 5 shows the correlation between the absorbance of BLG-RGO dispersions at 266 nm and the concentration of β-lactoglobulin. It can be seen that the absorption intensity of BLG-RGO did not increase continuously with the increasing concentration of β-lactoglobulin. Instead, the absorption intensity increased initially and then reached a plateau region. So the optimum concentration for β-lactoglobulin can be determined as 0.5 mg/mL and we adopted this β-lactoglobulin concentration in the following studies.

Apart from the concentration of β-lactoglobulin, pH value of the solution is another important parameter for the dispersion result. As reported previously, β-lactoglobulin can exist in different pH-dependent structural states.[47] To understand the correlativity between the pH values and the stabilization of BLG-RGO dispersions, we adjusted the pH of BLG-RGO solutions from 2.0 to 12.0 using NaOH and HCl aqueous solution followed by a 10 min ultrasonication. Figure 6 shows

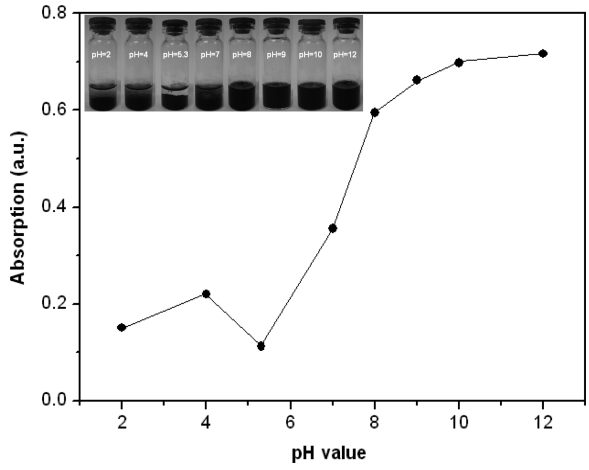

Figure 6. UV−vis absorption of BLG-RGO solutions (0.5 mg/mL β-lactoglobulin) at 266 nm with different pH values and the inset showing the photographs of BLG-RGO solutions at pH of 2.0, 4.0, 5.3, 7.0, 8.0, 9.0, 10.0, and 12.0.

the UV−vis absorption of different BLG-RGO solutions at 266 nm, and the absorption intensity increases with increasing pH values. The inset shows the photographs of BLG-RGO solutions with different pH values at 2.0, 4.0, 5.3, 7.0, 8.0, 9.0, 10.0, and 12.0. It is obvious that the BLG-RGO dispersion can only be stable at the alkaline range and the absorption almost unchanged as the pH varies from 9.0 to 12.0. Also the isoelectric point should be avoided during the dispersing process, and the absorption of BLG-RGO solution with pH 5.3 is the lowest. We attribute this phenomenon to the different conformation and hydrophilic groups of β-lactoglobulin at pH values. With the pH value from 2.0 to 12.0, β-Lactoglobulin undergoes the dimer-to-monomer conformation transition and more unfolded structures are exposed to the solvent. When the pH value reaches to 9.0, 80% of the amino acid residues of β-lactoglobulin can be accessible to the solvent, resulting in increased hydrophilicity of β-lactoglobulin. So the obtained

dx.doi.org/10.1021/am300634n | ACS Appl. Mater. Interfaces 2012, 4, 3278−3284

BLG-RGO composite can be dispersed better in water with a pH value more than 9.0.

The β-lactoglobulin could also promote the reduction process and enhance the quality of RGO, since the graphene sheets maintain an individual and flat state during the reduction process by the aid of β-lactoglobulin. The crystal structure of graphite is damaged during the preparation of GO through Hummers method. While after the reduction process, RGO is partially restored to the ordered crystal structure and the C atoms are transformed from sp^3 to sp^2. Raman spectroscopy was performed to distinguish the ordered and disordered structure of graphite. Figure 7 shows the Raman spectra of GO, RGO, and BLG-RGO with the G-band peaks at ~1600 cm^{-1} and D-band peaks at ~1340 cm^{-1}. The G-band arises from the vibration of sp^2 C atoms and the D-band represents the disorder and defect intensity of the crystal structure, herein indicating the reduction degree.[48,49] The intensity ratio of D and G band (I_D/I_G) can be used to quantify the relative content of defects and the sp^2 domain size. The obtained I_D/I_G for GO is about 1.18, indicating a decrease in the average size of sp^2 C atoms and an increase of defects due to the extensive oxidation and ultrasonication exfoliation.[50] In contrast, after the hydrazine reduction, the RGO exhibits an I_D/I_G ratio of 1.37, which implies more defects have been introduced onto the RGO sheets.[51] While for the BLG-RGO sample, the I_D/I_G ratio reduces to 1.29. The reason may be that the graphene sheets became somewhat flatter in the reduction process by β-lactoglobulin. That is, the β-lactoglobulin improves the evolution of sp^3 to sp^2 structure and promotes the restore of the crystal structure, resulting in a deeper reduction degree. This result can further verify the previous observation in UV–vis spectra.

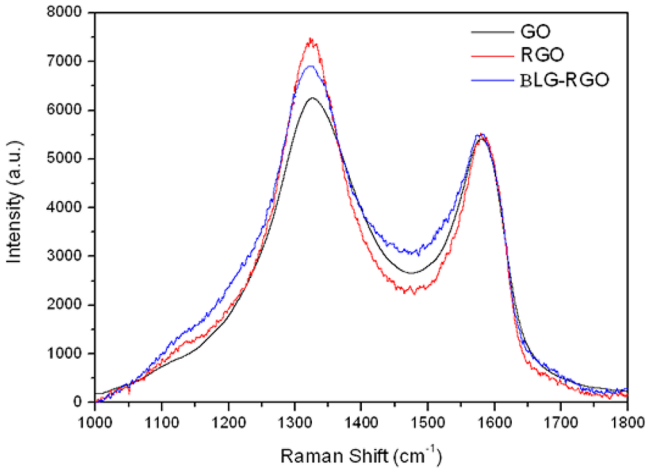

Figure 7. Raman spectra taken at 633 nm of GO (black curve), RGO (red curve), and BLG-RGO (blue curve).

Assembly and Application of Au Nanoparticles Based on BLG-RGO Composite. β-Lactoglobulin contains two disulfide bonds and one free sulfhydryl group.[52] With the adsorption of β-Lactoglobulin on graphene, many sulfhydryl groups are introduced onto the surface of BLG-RGO composite, which may provide many active sites to anchor nanoparticles. As an example, the BLG-RGO composite were further used as template for Au nanoparticles assembly. The general structure of β-lactoglobulin and the synthesis of BLG-RGO/Au hybrid have been given in Scheme 1. After the addition of gold precursor and reducing agent to the BLG-RGO dispersion, the BLG-RGO/Au hybrid can be obtained immediately. Figure 8a shows the TEM images of Au nanoparticles based on BLG-RGO composite and the inset shows a higher resolution TEM image of the same sample to provide more details of the gold structure. The obtained Au spherical particles are homogeneous distributed over the whole surface of BLG-RGO sheets with a relatively average size about 20 nm.

Scheme 1. (a) Structure of β-Lactoglobulin and (b) the Synthesis of BLG-RGO/Au Hybrid

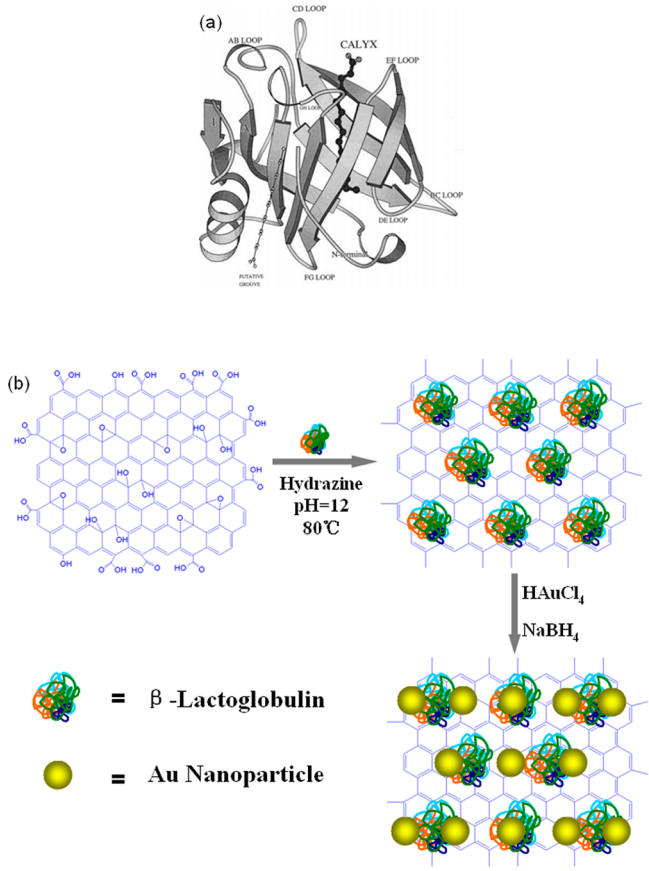

Au nanostructures, especially the nanoparticles, can be used as the substrate for SERS.[53−56] According to our previous report, the Au nanoparticle patterns as the SERS substrate can give an enhancement factor of 7.28×10^4.[53] It would be interesting to explore whether the Au nanoparticles based on BLG-RGO composite could be used for fabricating intense and stable SERS substrates. As shown in Figure 8b, R6G on the quartz substrate and the BLG-RGO composite substrate both gave very weak signals; however, R6G on the BLG-RGO/Au hybrid substrate gave a relatively stronger response. Apparently, vibrations at 1185, 1310, 1361, 1507, and 1646 cm^{-1}, which are assigned to C–H in-plane bending, C–O–C stretching and C–C stretching of the aromatic ring, are enhanced greatly.[57,58] The surface enhancement factors (EF) of R6G on the pattern film were calculated using the expression

$$EF = (I_{SERS}/N_{ads})/(I_{bulk}/N_{bulk}) \quad (1)$$

where I_{SERS} is the intensity of a vibrational mode in the surface enhanced spectrum, I_{bulk} is the intensity of the same mode in the Raman spectrum, N_{ads} is the number of molecules adsorbed

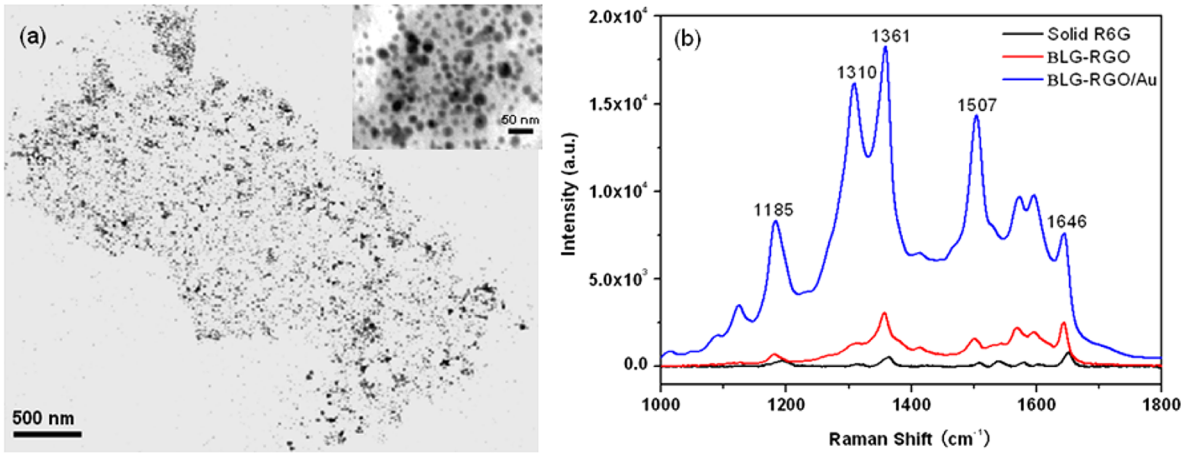

Figure 8. (a) TEM images of BLG-RGO/Au hybrid and the inset showing a higher resolution TEM image of the same sample. (b) Raman spectra of solid R6G (black curve) and SERS spectra on BLG-RGO (red curve) and BLG-RGO/Au hybrid (blue curve).

on the SERS-active substrate, and N_{bulk} is the number of molecules sampled in the bulk. The EF for the BLG-RGO/Au nanoparticles at 1185 and 1361 cm^{-1} can be calculated to be 4.48×10^5 and 4.83×10^5, respectively. These EF data indicate the as-prepared Au nanoparticles based on BLG-RGO composite have high efficiency as SERS substrates and might have potential applications in SERS-based technology.

CONCLUSION

In summary, we have demonstrated that RGO sheets can be readily decorated by β-lactoglobulin and the obtained BLG-RGO composite can be dispersed in aqueous solution with pH-sensitive solubility. In addition, β-lactoglobulin can also promote the reduced process of GO by hydrazine, resulting in a more ordered graphite crystal structure. Moreover, the BLG-RGO composite is an efficient platform for Au nanoparticles self-assembly and the resulting BLG-RGO/Au hybrid has high efficiency as SERS substrate.

AUTHOR INFORMATION

Corresponding Author

*E-mail: lqzheng@sdu.edu.cn. Phone number: +86-531-88366062. Fax: +86-531-885647.

Notes

The authors declare no competing financial interest.

ACKNOWLEDGMENTS

The authors are grateful to the National Natural Science Foundation of China (No. 50972080 and No. 91127017), National Basic Research Program (2009CB930101).

REFERENCES

(1) Novoselov, K. S.; Geim, A. K.; Morozov, S. V.; Jiang, D.; Zhang, Y.; Dubonos, S. V.; Grigorieva, I. V.; Firsov, A. A. *Science* **2004**, *306*, 666−669.
(2) Allen, M. J.; Tung, V. C.; Kaner, R. B. *Chem. Rev.* **2010**, *110*, 132−145.
(3) Geim, A. K. *Science* **2009**, *324*, 1530−1534.
(4) Rao, C. N. R.; Sood, A. K.; Subrahmanyam, K. S.; Govindaraj, A. *Angew. Chem., Int. Ed.* **2009**, *48*, 7752−7777.
(5) Sutter, P. W.; Flege, J. I.; Sutter, E. A. *Nat. Mater.* **2008**, *7*, 406−411.
(6) Emtsev, K. V.; Bostwick, A.; Horn, K.; Jobst, J.; Kellogg, G. L.; Ley, L.; McChesney, J. L.; Ohta, T.; Reshanov, S. A.; Röhrl, J.; Rotenberg, E.; Schmid, A. K.; Waldmann, D.; Weber, H. B.; Seyller, T. *Nat. Mater.* **2009**, *8*, 203−207.
(7) Kim, K. S.; Zhao, Y.; Jang, H.; Lee, S. Y.; Kim, J. M.; Kim, K. S.; Ahn, J. H.; Kim, P.; Choi, J. Y.; Hong, B. H. *Nature* **2009**, *457*, 706−710.
(8) Li, X. S.; Cai, W. W.; An, J. H.; Kim, S.; Nah, J.; Yang, D. X.; Piner, R.; Velamakanni, A.; Jung, I.; Tutuc, E.; Banerjee, S. K.; Colombo, L.; Ruoff, R. S. *Science* **2009**, *324*, 1312−1314.
(9) Hong, W.; Xu, Y.; Lu, G.; Li, C.; Shi, G. *Electrochem. Commun.* **2008**, *10*, 1555−1558.
(10) Li, X.; Wang, X.; Zhang, L.; Lee, S.; Dai, H. *Science* **2008**, *319*, 1229−1232.
(11) Yoo, E.; Kim, J.; Hosono, E.; Zhou, H.; Kudo, T.; Honma, I. *Nano Lett.* **2008**, *8*, 2277−2282.
(12) Bunch, J. S.; van der Zande, A. M.; Verbridge, S. S.; Frank, I. W.; Tanenbaum, D. M.; Parpia, J. M.; Craighead, H. G.; McEuen, P. L. *Science* **2007**, *315*, 490−493.
(13) Yang, M. H.; Choi, B. G.; Park, T. G. *Nanoscale* **2011**, *3*, 2950−2956.
(14) Patil, A. J.; Vickery, J. L.; Scott, T. B.; Mann, S. *Adv. Mater.* **2009**, *21*, 3159−3164.
(15) Park, S.; Ruoff, R. S. *Nat. Nanotechnol* **2009**, *4*, 217−224.
(16) Yang, X. Y.; Zhang, X. Y.; Ma, Y. F.; Huang, Y. *J. Mater. Chem.* **2009**, *19*, 2710−2714.
(17) Yang, H. F.; Shan, C. S.; Li, F. H.; Han, D. X.; Zhang, Q. X. *Chem. Commun.* **2009**, *26*, 3880−3882.
(18) Si, Y. C.; Samulski, E. T. *Nano Lett.* **2008**, *8*, 1679−1682.
(19) Hsiao, M. C.; Liao, S. H.; Yen, M. Y.; Liu, P. I.; Pu, N. W.; Wang, C. N.; M. Ma, C. C. *ACS Appl. Mater. Interfaces* **2010**, *2*, 3092−3099.
(20) Das, S.; Wajid, A. S.; Shelburne, J. L.; Liao, Y. C.; Green, M. J. *ACS Appl. Mater. Interfaces* **2011**, *3*, 1844−1851.
(21) Lotya, M.; Hernandez, Y.; King, P. J.; Smith, R. J.; Nicolosi, V.; Karlsson, L. S.; Blighe, F. M.; Wang, Z. M.; McGovern, I. T.; Duesberg, G. S.; Coleman, J. N. *J. Am. Chem. Soc.* **2009**, *131*, 3611−3620.
(22) Liang, Y. Y.; Wu, D. Q.; Feng, X. L.; Műllen, K. *Adv. Mater.* **2009**, *21*, 1679−1683.
(23) Li, F. H.; Bao, Y.; Chai, J.; Zhang, Q. X.; Han, D. X.; Niu, L. *Langmuir* **2010**, *26*, 12314−12320.
(24) Cai, X.; Tan, S. Z.; Lin, M. S.; Xie, A.; Mai, W. J.; Zhang, X. J.; Lin, Z. D.; Wu, T.; Liu, Y. L. *Langmuir* **2011**, *27*, 7828−7835.
(25) Kim, T. Y.; Lee, H. W.; Kim, J. E.; Suh, K. S. *ACS Nano* **2010**, *4*, 1612−1618.
(26) Zhou, X. S.; Wu, T. B.; Ding, K. L.; Hu, B. J.; Hou, M. Q.; Han, B. X. *Chem. Commun.* **2010**, *46*, 386−388.
(27) Seo, J. T.; Green, A. A.; Antaris, A. L.; Hersam, M. C. *J. Phys. Chem. Lett.* **2011**, *2*, 1004−1008.

(28) Liu, J. B.; Fu, S. H.; Yuan, B.; Li, Y. L.; Deng, Z. X. *J. Am. Chem. Soc.* **2010**, *132*, 7279−7281.
(29) Yang, F.; Liu, Y. Q.; Gao, L.; Sun, J. *J. Phys. Chem. C* **2010**, *114*, 22085−22091.
(30) Viseu, M. I.; Carvalho, T. I.; Costa, S. *Biophys. J.* **2004**, *86*, 2392−2402.
(31) Fragneto, G.; Su, T. J.; Lu, J. R.; Thomas, R. K.; Rennie, A. R. *Phys. Chem. Chem. Phys.* **2000**, *2*, 5214−5221.
(32) Tomoaki, H.; Takaharu, S.; Hisahiko, W. *Langmuir* **2009**, *25*, 226−234.
(33) Hummers, W. S.; Offeman, R. E. *J. Am. Chem. Soc.* **1958**, *80*, 1339.
(34) Lerf, A.; He, H. Y.; Forster, M.; Klinowski, J. *J. Phys. Chem. B* **1998**, *102*, 4477−4482.
(35) Szabo, T. *Chem. Mater.* **2006**, *18*, 2740−2749.
(36) Stankovich, S.; Dikin, D. A.; Piner, R. D.; Kohlhaas, K. A.; Kleinhammes, A.; Jia, Y.; Wu, Y.; Nguyen, S. T.; Ruoff, R. S. *Carbon* **2007**, *45*, 1558−1565.
(37) Li, D.; Müller, M. B.; Gilje, S.; Kaner, R. B.; Wallace, G. G. *Nat. Nanotechnol.* **2008**, *3*, 101.
(38) Kim, J.; Cote, L. J.; Kim, F.; Huang, J. X. *J. Am. Chem. Soc.* **2010**, *132*, 260−267.
(39) Vijayalakshmi, L.; Krishna, R.; Sankaranarayanan, R.; Vijayan, M. *Proteins* **2007**, *71*, 241−249.
(40) Kesley, M. G. O.; Vera, L.; Michelle, M.; Lindsay, S.; Igor, P. *Eur. J. Biochem.* **2001**, *268*, 477−483.
(41) Wu, S. Y.; Pérez, M. D.; Puyol, P.; Sawyer, L. *J. Biol. Chem.* **1999**, *274*, 170−174.
(42) Jeong, H. K.; Lee, Y. P.; Lahaye, R.; Park, M. H.; An, K. H.; Kim, I. J.; Yang, C. W.; Park, C. Y.; Ruoff, R. S.; Lee, Y. H. *J. Am. Chem. Soc.* **2008**, *130*, 1362−1366.
(43) Titelman, G. I.; Gelman, V.; Bron, S.; Khalfin, R. L.; Cohen, Y.; BiancoPeled, H. *Carbon* **2005**, *43*, 641−649.
(44) Beauchemin, R.; Soukpoe-Kossi, C. N.; Thomas, T. J.; Carpentier, R.; Tajmir-Riahi, H. A. *Biomacromolecules* **2008**, *8*, 3177−3183.
(45) Krimm, S.; Bandekar. *J. Adv. Protein. Chem.* **1986**, *38*, 181−364.
(46) Paredes, J. I.; Villar-Rodil, S.; Martinez-Alonso, A.; Tascon, J. M. D. *Langmuir* **2008**, *24*, 10560−10564.
(47) Taulier, T.; Chalikian, T. V. *J. Mol. Biol.* **2001**, *314*, 873−889.
(48) Eda, G.; Chhowalla, M. *Adv. Mater.* **2010**, *22*, 2392−2415.
(49) Dresselhaus, M. S.; Jorio, A.; Hofmann, M.; Dresselhaus, G.; Saito, S. *Nano Lett.* **2010**, *10*, 751−758.
(50) Zhang, W. N.; He, W.; Jing, X. L. *J. Phys. Chem. B* **2010**, *114*, 10368−10373.
(51) Mohanty, N.; Nagaraja, A.; Armesto, J.; Berry, V. *Small* **2010**, *6*, 226−231.
(52) Sakai, K.; Sakurai, K.; Sakai, M. *Protein Sci.* **2000**, *9*, 1719−1729.
(53) Bai, X. T.; Li, X. W.; Zheng, L. Q. *Langmuir* **2010**, *26*, 12209−12214.
(54) Jia, H.; Bai, X. T.; Li, N.; Yu, L.; Zheng, L. Q. *CrystEngComm* **2011**, *13*, 6179−6184.
(55) Huang, D. P.; Bai, X. T.; Zheng, L. Q. *J. Phys. Chem. C* **2011**, *115*, 14641−14647.
(56) Huang, T.; Meng, F.; Qi, L. M. *Langmuir* **2010**, *26*, 7582−7589.
(57) Joseph, D.; Geckeler, K. E. *Langmuir* **2009**, *25*, 13224−13231.
(58) Guo, S. J.; Dong, S. J.; Wang, E. K. *Cryst. Growth Des.* **2009**, *9*, 372−377.